

Antiferromagnetic to ferromagnetic phase transition as a transition to partial ordered spins. Application to $La_{1-x}Ca_xMnO_3$ in the doping range $x \geq 0.50$.

N. Karchev

Department of Physics, Sofia University, James Bourchier 5 blvd., 1164 Sofia, Bulgaria

Abstract

Magnetic state is a partial ordered state if only part of the electrons in the system give contribution to the magnetic order. We study Heisenberg model of two sublattice spin system, on the body-centered cubic lattice, with antiferromagnetic nearest neighbors exchange of sublattice A and B spins and two different ferromagnetic exchange constants for sublattice A (J^A) and B (J^B) spins. When $J^A > J^B$ the system undergoes transition from paramagnetism to ferromagnetism at Curie temperature T_C . Only the sublattice A spins give contribution to the magnetization of the system. Upon cooling, the system possesses ferromagnetism to antiferromagnetism transition at Néel temperature $T_N < T_C$. Below T_N sublattice A and B electrons give contribution to the magnetization. The transition is a partial ordered transition. There is thermodynamic evidence for this transition in the magnetic specific heat of the system. As a function of temperature there are two maxima. At high temperature T_C it is λ -type. At lower temperature T_N it characterizes the transition from ferromagnetism to antiferromagnetism. As an example of ferromagnetism to antiferromagnetism partial ordered transition we consider the material $La_{1-x}Ca_xMnO_3$ in the doping range $x \geq 0.50$. Our calculations reproduce the experimental magnetization-temperature curve.

Keywords: ferromagnetism, antiferromagnetism, transition
75.50.Gg, 71.70.Ej, 75.10.Dg, 75.10.Lp

Email address: naoum@phys.uni-sofia.bg ()

1. Introduction

The ferromagnetic to antiferromagnetic (FM-AFM) phase transition is unusual phenomenon. There are various reasons causing the FM-AFM transition. Experimental results and Density-functional theory calculations show an electrically manipulated FM to AFM transition in van der Waals ferromagnet $Cr_{1.2}Te_2$ [1]. Several experiments show FM-AFM transition driven by pressure. The contraction of the crystal under various pressures is discussed in relation to FM - AFM transition [2]. In the single crystal of $LaCrGe_3$, increasing pressure, ferromagnetic quantum criticality is avoided by appearance of FM to AFM transition[3, 4].

Perhaps the most are the experiments with chemical substitution. The FM-AFM transition in $La_{1-x}Y_xMn_2Si_2(^{57}Fe)$ compounds is realized at $x_{cr} = 0.15$. It is a result of a change in the exchange interaction linked with changes in interatomic distances [5]. The nature of the ferromagnetic-antiferromagnetic transition in $Y_{1-x}La_xTiO_3$ for $x < 0.3$ is reported in [6]. The authors claim that the thermal phase transition does not show conventional second-order behavior. Cuprate $(La - R)_4Ba_2Cu_2O_{10}$ shows FM-AFM transition by replacing La ions with rare earth ($R = Nd, Sm, Eu, Gd$) [7].

Another material that possesses FM-AFM transition is $Pr_{1-x}Gd_xB_4$ [8]. The evolution of the antiferromagnetic correlation between the magnetic moments of Pr and Gd breaks the ferromagnetic order of Pr . The experiments suggest that theoretically one has to consider two spins Heisenberg model. The temperature dependence of the magnetic specific heat of $Pr_{1-x}Gd_xB_4$ shows the main peak that corresponds to the transition from paramagnetic to ordered phase, is λ -type, indicating that the transition is of second order. The specific heat of $Pr_{1-x}Gd_xB_4$ at ($x=0.2$) shows additional two peaks. They correspond to the FM-AFM transition and suggest that the transition is of first order.

Review of the FM-AFM transition in the Heusler alloy series $Pd_2MnSn_xIn_{1-x}$ is provided in [9]. Magnetic moments are localized on the Mn sites. The parent compound Pd_2MnSn is a ferromagnetic with Curie temperature $T_C = 189K$. The Mn moment is $4.1\mu_B$ per atom which means that the valent state is Mn^{3+} . As Sn is replaced by In the alloy becomes multi valent and undergoes ferromagnetic to antiferromagnetic transition when Sn concentration "x" is between 0.65 and 0.45.

The evolution of magnetism in the $UIr_{1-x}Rh_xGe$ alloy system is investigated in [10]. The system is ferromagnetic at $x = 0.86$ and $x = 0.57$. The system possesses FM-AFM transition at $x = 0.55$ demonstrated by acute fall of magnetization at Néel temperature. The Néel temperature increases with decrease of Rh concentration.

We focus our attention on FM-AFM transition accompanied with transition to charge order state. The real space ordering of charge carriers in crystal occurs when Coulomb interaction overcomes the kinetic energy of carriers. The perovskite-type manganese oxide, $Pri_{1-x}Sr_xMnO_3$ at ($x = 0.5$), shows simultaneous first-order phase transition from a ferromagnetic (FM) metal to antiferromagnetic (AFM) nonmetal at 140 K and charge ordering [11].

The effect of the doping on the phase transition is more prominent in the experiments with $La_{1-x}Ca_xMnO_3$ [12]. Magnetic moments are localized on the Mn sites[13]. The manganese has an incomplete $3d$ shell with four or three electrons for Mn^{3+} and Mn^{4+} respectively. Due to the crystal field splitting effect, the degeneracy of the five $3d$ orbitals is lifted and they are grouped into one triplet t_{2g} and one doublet e_g . The triplet has lower energy because of the space orientation of the corresponding orbitals inside the octahedron of six oxygen ions, surrounding the central manganese ion. The population of the t_{2g} electrons remains constant and the Hund rule enforces alignment of the t_{2g} spins into a state of maximum spin $s = 3/2$. Then the t_{2g} sector can be replaced by a localized spin at each manganese ion, reducing the complexity of the original five orbital model. The electrons from the e_g sector however can move from ion to ion, maintaining the projection of their spin, and are called mobile electrons. The only important interaction between the two sectors is the Hund coupling between localized t_{2g} spins and mobile e_g electrons. Increasing the doping "x" the density of e_g electrons decreases and charge order state emerges. At $x = 0.5$ the system undergoes FM-AFM transition and all e_g electrons have occupied one off the antiferromagnetic sublattices. When $x = 1$, the final compound is spin 3/2 antiferromagnetic $CaMnO_3$.

The theoretical studies of FM-AFM transition are considerably less. Universal quantum effects are used within extended Landau theory to explain the FM-AFM transition[14]. On the other hand, it is shown that microscopic properties of specific materials trigger such transition. Effective models incorporating these properties are suitable tools to study magnetic properties of the materials. Low energy model of USb_2 is derived to study the FM-AFM transition [15]. Novel mechanism of FM-AFM transition is proposed[16] to

explain the experimentally observed pressure induced transition in $LaCrGe_3$ as a mechanism to avoid the ferromagnetic quantum criticality[3, 4].

In the present article we consider FM-AFM transition as a partial ordered transition. Magnetic state is a partial ordered state if only part of the electrons in the system give contribution to the magnetic order. It is studied in exactly solvable models [17, 18, 19], by means of Green's function approach [20] and utilizing the Monte Carlo method [18]. A modified spin-wave theory of magnetism has been developed to investigate the state of partial order in spin-fermion systems [6] and field-cooled ferrimagnetic spinels [22]. In the present paper, we use this theory to study the transition from antiferromagnetism to ferromagnetism in $La_{1-x}Ca_xMnO_3$ in the doping range $x \geq 0.50$. It is proved that this transition is partial order one. The phase diagram of $La_{1-x}Ca_xMnO_3$ in the doping range $x < 0.50$ is theoretically studied in [13].

2. Model

We consider Heisenberg model of two sublattice spin system with antiferromagnetic nearest neighbors exchange (J) of sublattice A and B spins and two different ferromagnetic exchange constants for sublattice A (J^A) and B (J^B) spins. The Hamiltonian of the system is

$$\begin{aligned}
 H = & J \sum_{\langle ij \rangle} \mathbf{S}_i^A \cdot \mathbf{S}_j^B \\
 & - J^A \sum_{\langle\langle ij \rangle\rangle_A} \mathbf{S}_i^A \cdot \mathbf{S}_j^A - J^B \sum_{\langle\langle ij \rangle\rangle_B} \mathbf{S}_i^B \cdot \mathbf{S}_j^B
 \end{aligned} \tag{1}$$

where ($\mathbf{S}^A, \mathbf{S}^B$) are spin $s = 3/2$ operators, the sums are over all sites of a body-centered cubic (bcc) lattice. To be specific we choose ($J^A > J^B$). We introduce Holstein-Primakoff representation for the spin operators $\mathbf{S}_i^A(a^+, a)$ and $\mathbf{S}_i^B(b^+, b)$. Rewriting the effective Hamiltonian in terms of the Bose operators (a^+, a, b^+, b) we keep only the quadratic and quartic terms. The next step is to represent the Hamiltonian in the Hartree-Fock (HF) approximation, with temperature-dependent HF parameters to be determined self consistently:

$$H \approx H_{HF} = H_{cl} + H_q, \tag{2}$$

where

$$\begin{aligned}
 H_{cl} = & 6NJ^A s^2 (u^A - 1)^2 + 6NJ^B s^2 (u^B - 1)^2 \\
 & + 8NJs^2 (u - 1)^2,
 \end{aligned} \tag{3}$$

and

$$H_q = \sum_{k \in B_r} \left[\varepsilon_k^a a_k^+ a_k + \varepsilon_k^b b_k^+ b_k - \gamma_k (a_k^+ b_k^+ + b_k a_k) \right], \quad (4)$$

with $N = N^A = N^B$ is the number of sites on a sublattice. The two equivalent sublattices A and B of the bcc lattice are simple cubic lattices. The wave vector k runs over the reduced first Brillouin zone B_r of a bcc lattice which is the first Brillouin zone of a simple cubic lattice.

The dispersions are given by equalities

$$\begin{aligned} \varepsilon_k^a &= 4sJ^A u^A (3 - \cos k_x - \cos k_y - \cos k_z) + 8sJu \\ \varepsilon_k^b &= 4sJ^B u^B (3 - \cos k_x - \cos k_y - \cos k_z) + 8sJu \\ \gamma_k &= 8Jus \cos \frac{k_x}{2} \cos \frac{k_y}{2} \cos \frac{k_z}{2} \end{aligned} \quad (5)$$

The equations (35) show that Hartree-Fock parameters (u^A, u^B, u) renormalize the intra and inter-sublattice exchange constants (J^A, J^B, J) respectively.

To diagonalize the Hamiltonian one introduces new Bose fields $\alpha_k, \alpha_k^+, \beta_k, \beta_k^+$ by means of Bogoliubov transformation for Bose system:

$$\begin{aligned} a_k &= u_k \alpha_k + v_k \beta_k^+ & a_k^+ &= u_k \alpha_k^+ + v_k \beta_k \\ b_k &= u_k \beta_k + v_k \alpha_k^+ & b_k^+ &= u_k \beta_k^+ + v_k \alpha_k, \end{aligned} \quad (6)$$

where the coefficients of the transformation u_k and v_k are real functions of the wave vector k :

$$\begin{aligned} u_k &= \sqrt{\frac{1}{2} \left(\frac{\varepsilon_k^a + \varepsilon_k^b}{\sqrt{(\varepsilon_k^a + \varepsilon_k^b)^2 - 4\gamma_k^2}} + 1 \right)} \\ v_k &= \text{sign}(\gamma_k) \sqrt{\frac{1}{2} \left(\frac{\varepsilon_k^a + \varepsilon_k^b}{\sqrt{(\varepsilon_k^a + \varepsilon_k^b)^2 - 4\gamma_k^2}} - 1 \right)}. \end{aligned} \quad (7)$$

The transformed Hamiltonian adopts the form

$$H_q = \sum_{k \in B_r} \left(E_k^\alpha \alpha_k^+ \alpha_k + E_k^\beta \beta_k^+ \beta_k + E_k^0 \right), \quad (8)$$

with new dispersions

$$\begin{aligned}
E_k^\alpha &= \frac{1}{2} \left[\sqrt{(\varepsilon_k^a + \varepsilon_k^b)^2 - 4\gamma_k^2} - \varepsilon_k^b + \varepsilon_k^a \right] \\
E_k^\beta &= \frac{1}{2} \left[\sqrt{(\varepsilon_k^a + \varepsilon_k^b)^2 - 4\gamma_k^2} + \varepsilon_k^b - \varepsilon_k^a \right]
\end{aligned} \tag{9}$$

and vacuum energy

$$E_k^0 = \frac{1}{2} \left[\sqrt{(\varepsilon_k^a + \varepsilon_k^b)^2 - 4\gamma_k^2} - \varepsilon_k^b - \varepsilon_k^a \right] \tag{10}$$

The wave vector k runs over the reduced first Brillouin zone B_r of a bcc lattice .

For positive values of the Hartree-Fock parameters and all values of $k \in B_r$, the dispersions are nonnegative $E_k^\alpha \geq 0$, $E_k^\beta \geq 0$. The α_k and β_k bosons are the long-range (**magnon**) excitations in the system with antiferromagnetic dispersion $E_k^\alpha \propto c^\alpha |k|$ and $E_k^\beta \propto c^\beta |k|$, near the zero wave vector[23]. For spin velocity constants we obtained

$$c^\alpha = c^\beta = 4s\sqrt{Ju(J^A u^A + J^B u^B + Ju)}. \tag{11}$$

The free energy of a system with Hamiltonian H_{HF} equations (32), (33) and (34) is

$$\begin{aligned}
\mathcal{F} &= 6NJ^A s^2 (u^A - 1)^2 + 6NJ^B s^2 (u^B - 1)^2 \\
&+ 8NJs^2 (u - 1)^2 + \frac{1}{N} \sum_{k \in B_r} E_k^0 \\
&+ \frac{1}{\beta N} \sum_{k \in B_r} \left[\ln(1 - e^{-\beta E_k^\alpha}) + \ln(1 - e^{-\beta E_k^\beta}) \right],
\end{aligned} \tag{12}$$

where $\beta = 1/T$ is the inverse temperature, with Boltzmann constant k_B set equal to 1 . Then, the system of equations for the Hartree-Fock parameters is

$$\partial\mathcal{F}/\partial u^A = 0, \quad \partial\mathcal{F}/\partial u^B = 0, \quad \partial\mathcal{F}/\partial u = 0. \tag{13}$$

One can write them by means of the Bose functions n_k^α and n_k^β of α and β excitations [23].

The Hartree-Fock parameters are positive functions of T/J , solution of the system of equations (42). Utilizing these functions, one can calculate the spontaneous magnetization on the two sublattices

$$M^A = \langle S_j^{A3} \rangle \quad j \text{ is from sublattice } A \quad (14)$$

$$M^B = \langle S_j^{B3} \rangle \quad j \text{ is from sublattice } B$$

and $M = M^A + M^B$, the spontaneous magnetization of the system. In terms of the Bose functions

$$M^A = s - \frac{1}{N} \sum_{k \in B_r} \left[u_k^2 n_k^\alpha + v_k^2 n_k^\beta + v_k^2 \right] \quad (15)$$

$$M^B = -s + \frac{1}{N} \sum_{k \in B_r} \left[v_k^2 n_k^\alpha + u_k^2 n_k^\beta + v_k^2 \right],$$

where u_k and v_k are functions of the wavevector k , Bogoliubov coefficients in the transformation [23].

We utilize the solutions of HP parameters as a functions of temperature to calculate the sublattice A and B magnetizations. The magnon excitations - α_k and β_k are complicated mixtures of the transversal fluctuations of the A and B spins. As a result the magnons' fluctuations suppress in a different way the magnetization on sublattices A and B. Quantitatively this depends on the exchange constants J^A and J^B . At characteristic temperature T_N spontaneous magnetization on sublattice B becomes equal to zero, while spontaneous magnetization on sublattice A is still nonzero[23]. The total magnetization $M^A + M^B$ increases and reaches its maximum value at T_N . The system in the temperature interval $(0, T_N)$ has two antiferromagnetic magnons but sublattice A and B magnetizations do not compensate each other. We call this phase noncompensated antiferromagnetic.

Above the Néel temperature the magnetic moments of the sublattice B electrons do not contribute the magnetization of the system. Only sublattice A electrons do. To study this "partial order" we make use of the Takahashi modified spin-wave theory [5, 6, 22] and introduce two parameters λ^A and λ^B to enforce the magnetization on the two sublattices to be equal to zero in paramagnetic phase. The new Hamiltonian is obtained from the original one by adding two new terms:

$$\hat{H} = H - \sum_{i \in A} \lambda^A S_i^{A3} + \sum_{i \in B} \lambda^B S_i^{B3} \quad (16)$$

In momentum space the new Hamiltonian adopts the form

$$\hat{H} = \sum_{k \in B_r} [\hat{\varepsilon}_k^a a_k^+ a_k + \hat{\varepsilon}_k^b b_k^+ b_k - \gamma_k (b_k a_k + b_k^+ a_k^+)] \quad (17)$$

where the new dispersions are

$$\hat{\varepsilon}_k^a = \varepsilon_k^a + \lambda^A, \quad \hat{\varepsilon}_k^b = \varepsilon_k^b + \lambda^B. \quad (18)$$

It is convenient to represent the parameters λ^A and λ^B in the form

$$\lambda^A = 8Jus(\mu^A - 1), \quad \lambda^B = 8Jus(\mu^B - 1). \quad (19)$$

The dispersions $\hat{\varepsilon}_k^a$ and $\hat{\varepsilon}_k^b$ adopt the form

$$\hat{\varepsilon}_k^a = 4sJ^A u^A (3 - \cos k_x - \cos k_y - \cos k_z) + 8sJu\mu^A \quad (20)$$

$$\hat{\varepsilon}_k^b = 4sJ^B u^B (3 - \cos k_x - \cos k_y - \cos k_z) + 8sJu\mu^B.$$

They are positive ($\hat{\varepsilon}_k^a > 0$, $\hat{\varepsilon}_k^b > 0$) for all values of the wavevector k , if the parameters μ^A and μ^B are positive ($\mu^A > 0$, $\mu^B > 0$).

To obtain the Hamiltonian (47) in diagonal form, we use the Bogoliubov transformation [23] replacing ε_k^a and ε_k^b with $\hat{\varepsilon}_k^a$ and $\hat{\varepsilon}_k^b$. The result is

$$\hat{H} = \sum_{k \in B_r} \left(\hat{E}_k^\alpha \alpha_k^+ \alpha_k + \hat{E}_k^\beta \beta_k^+ \beta_k + \hat{E}_k^0 \right), \quad (21)$$

where

$$\begin{aligned} \hat{E}_k^\alpha &= \frac{1}{2} \left[\sqrt{(\hat{\varepsilon}_k^a + \hat{\varepsilon}_k^b)^2 - 4\gamma_k^2} - \hat{\varepsilon}_k^b + \hat{\varepsilon}_k^a \right] \\ \hat{E}_k^\beta &= \frac{1}{2} \left[\sqrt{(\hat{\varepsilon}_k^a + \hat{\varepsilon}_k^b)^2 - 4\gamma_k^2} + \hat{\varepsilon}_k^b - \hat{\varepsilon}_k^a \right] \\ \hat{E}_k^0 &= \frac{1}{2} \left[\sqrt{(\hat{\varepsilon}_k^a + \hat{\varepsilon}_k^b)^2 - 4\gamma_k^2} - \hat{\varepsilon}_k^b - \hat{\varepsilon}_k^a \right] \end{aligned} \quad (22)$$

The dispersions Eq.(52) are well defined if square-roots in equations (52) are well defined. This is true if

$$\mu^A \mu^B \geq 1. \quad (23)$$

If $\mu^A \mu^B > 1$ the dispersions (52) are positive ($\hat{E}_k^\alpha > 0, \hat{E}_k^\beta > 0$). This means that the system is in paramagnetic phase. When $\mu^A \mu^B = 1$ the spectrum of the system possesses long-range (magnon) excitation and it is in ordered phase.

In the partial ordered phase above T_N with $M^B = 0$ sublattice A magnetization contributes the total magnetic moment. To study this ordered phase one has to solve a system of four equations, three for Hartree-Fock parameters and one ($M^B = 0$) for $\mu^A = 1/\mu^B$. The solution of the system, the Hartree-Fock parameters and parameters $\mu^A = 1/\mu^B$ as functions of T/J within interval $(0, T_C/J)$ are depicted in [23]. Above the T_C , the critical order-disorder transition temperature, one obtains $\mu^A \mu^B > 1$. The sublattice A and B magnetization M^A and M^B in partial ordered phase are depicted in [23]. The total magnetization $M^A + M^B$ is depicted in Fig.(1).

The figure for μ^A and μ^B [23] shows that μ^B is larger than μ^A . As a result we obtain that β excitation is gapped ($E_k^\beta > 0$ for all values of the wave vector k), while $E_0^\alpha = 0$ and near the zero wave vector

$$\hat{E}_k^\alpha \propto \hat{\rho} k^2 \quad (24)$$

with spin-stiffness constant

$$\begin{aligned} \hat{\rho} = & s \frac{(\mu^A + \mu^B)(J^A u^A + J^B u^B) + 2JU}{\mu^B - \mu^A} \\ & + sJ^A u^A - sJ^B u^B. \end{aligned} \quad (25)$$

This means that α_k boson is the long-range excitation (ferromagnetic magnon) in the system.

The sublattice A and B magnetizations are depicted as a function of dimensionless temperature T/J within the interval $(0, T_C/J)$, for a system with parameters $J^A/J = 0.8$ and $J^B/J = 0.006$ in figure (1). The figure shows that at T_N the system undergoes partial order transition from low temperature antiferromagnetic phase with $M^A > 0$ and $M^B < 0$, to high temperature ferromagnetic phase with $M^A > 0$ and $M^B = 0$.

By combining the calculations for the two phases, we obtain the total magnetization of the system as a function of temperature. As the temperature decreases, the onset of magnetism is at T_C . Below T_C the magnetization increases and reaches the maximum value at T_N . Below T_N magnetization decreases abruptly or smoothly depending on the parameters in the model and approaches zero. In the high temperature phase(T_N, T_C) the system

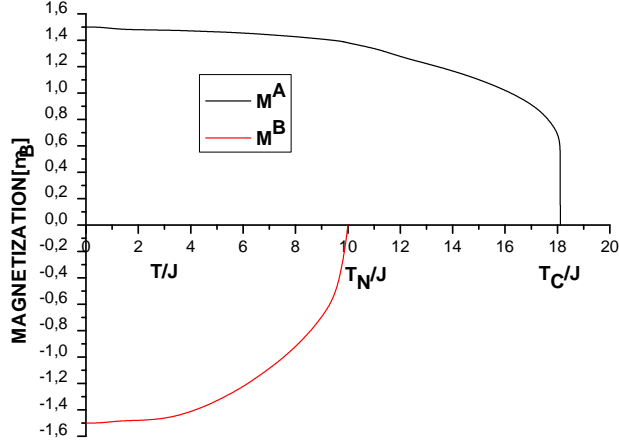


Figure 1: The sublattice A and B magnetization are depicted as a function of dimensionless temperature T/J within the interval $(0, T_C/J)$, for a system with parameters $J^A/J = 0.8$ and $J^B/J = 0.006$.

has one magnon with dispersion proportional to k^2 and the total magnetization is equal to the magnetization of sublattice A . The partial ordered phase is ferromagnetic. In the low temperature phase $(0, T_N)$ the system has two magnons with dispersion proportional to $|k|$ and the total magnetization $M = M^A + M^B$ is nonzero. The phase is noncompensated antiferromagnetic.

The curves for systems with parameters $(J^A/J = 0.8, J^B/J = 0.006)$ and $(J^A/J = 0.8, J^B/J = 0.6)$ are plotted in figure (2). They show that upon cooling the system has a transition from paramagnetic to ferromagnetic phase at T_{1C} and T_{2C} and at lower temperature T_{1N} and T_{2N} a transition from ferromagnetic to antiferromagnetic phase.

For the system (M_1) with a sublattice A exchange constant J^A much larger than J^B , the ferromagnetic "partial ordered" phase dominates. It is "partial ordered" phase because only sublattice A electrons contribute the magnetization of the system. Below T_{1N} the magnetization smoothly decreases and approaches zero. This phase is noncompensated antiferromagnetic and the system undergoes transition from ferromagnetic to noncompensated antiferromagnetic phase which is partial ordered transition.

For the system (M_2) the values of the exchange constants J^A and J^B

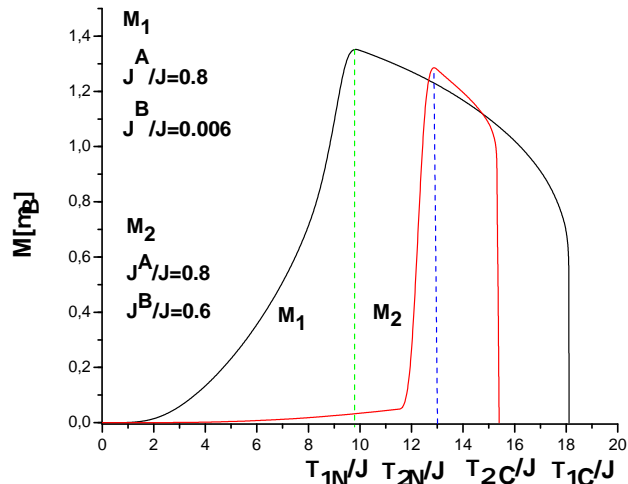


Figure 2: The magnetization $M^A + M^B$ are depicted, in units of μ_B , as a function of dimensionless temperature T/J for systems (M_1) with parameters $J^A/J = 0.8$, $J^B/J = 0.006$ and (M_2) with parameters $J^A/J = 0.8$, $J^B/J = 0.6$. The (M_1) system has a partial ordered transition from ferromagnetic to noncompensated antiferromagnetic phase at T_{1N}/J (green dash line). The (M_2) system has a partial ordered transition from ferromagnetic to antiferromagnetic phase at T_{2N}/J (blue dash line).

are very close. The low temperature phase $(0, T_{2N})$ dominates. All electrons of the system contribute the total magnetization which is zero. This means that the phase is antiferromagnetic, and at T_{2N} the system undergoes transition from antiferromagnetic to ferromagnetic phase. It is partial ordered transition.

An important feature of the FM-AFM transition is the magnetic specific heat of the system. The specific heat $C(T/J)$ as a function of dimensionless temperature T/J is depicted in figure (3). The function has two peaks. At T_C/J characterizes paramagnetic to ferromagnetic phase transition and at T_N/J the ferromagnetic to antiferromagnetic phase transition. At T_C/J , the order disorder transition is λ -type, suggesting that it is second order. The small shoulder below T_N/J indicates that it is of first order. In the compound $Pr_{1-x}Gd_xB_4$ the first-order transition is more expressively demonstrated by two peaks[8].

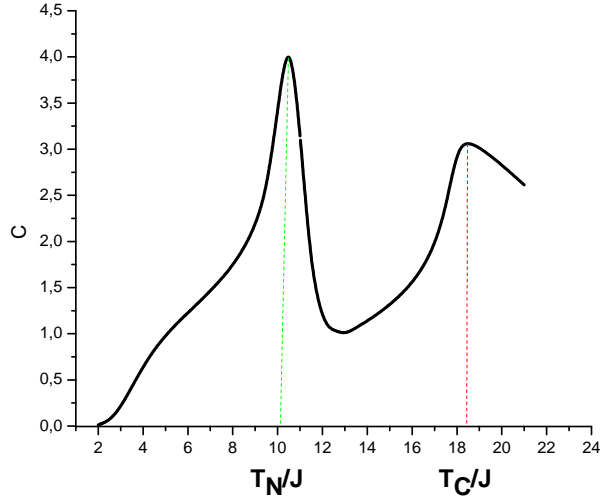


Figure 3: The magnetic specific heat is depicted as a function of dimensionless temperature T/J for a system with parameters $J^A/J = 0.8$ and $J^B/J = 0.006$. The high-temperature peak at T_C/J is a consequence of paramagnetic to ferromagnetic phase transition. It is λ -type second order transition. The peak at T_N/J characterizes the partial ordered ferromagnetic to noncompensated antiferromagnetic phase transition. The small shoulder below T_N is a sign for a first order transition

We apply the above developed theory of FM-AFM transition accompanied with transition to charge ordered state for $La_{1-x}Ca_xMnO_3$ in the doping range $x \geq 0.50$. At $x=0.5$, all the manganese ions that occupy the sites of the A sublattice are in the Mn^{3+} state, while those that occupy the sites in the B sublattice are in the Mn^{4+} state. The charge ordered state is in the heart of the FM-AFM transition. When $x=1$, i.e the density of charged electrons is zero, the system is spin $s = 3/2$ antiferromagnetic parent compound $CaMnO_3$. One can describe it by spin $3/2$ spin operators \mathbf{S}_i^A , \mathbf{S}_j^B and Heisenberg Hamiltonian of an antiferromagnetic system.

Within the interval $0.5 < x < 1$, all e_g electrons occupy the sites of the sublattice A, and by their averaging we obtain two additional spin-spin ferromagnetic exchange terms in the Heisenberg Hamiltonian with J^A exchange constant greater than J^B . As x increases, the density of e_g electrons decreases, therefore the effective exchange constants J^A and J^B decrease

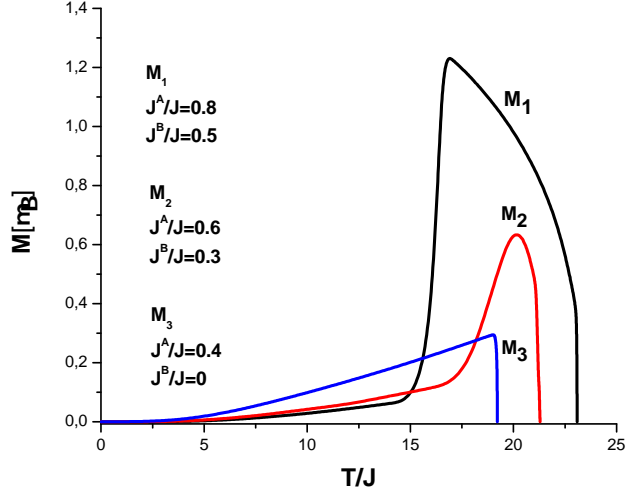


Figure 4: The magnetization-temperature curves are depicted in figure for systems: M_1 with parameters $J^A/J = 0.8$ and $J^B/J = 0.5$, M_2 with parameters $J^A/J = 0.6$ and $J^B/J = 0.3$ and M_3 with parameters $J^A/J = 0.4$ and $J^B/J = 0$. Compare with the experimentally measured magnetization temperature curves of $La_{1-x}Ca_xMnO_3$ [12] one obtains that M_1 curve reproduces to grate extend the experimental magnetization-temperature curve for $x = 0.50$, M_2 is in good agreement when $x = 0.52$ and M_3 qualitatively matches the experimental curve at $x = 0.55$.

preserving the inequality $J^A > J^B$.

We explore three systems, M_1 with parameters $J^A/J = 0.8$ and $J^B/J = 0.5$, M_2 with parameters $J^A/J = 0.6$ and $J^B/J = 0.3$ and M_3 with parameters $J^A/J = 0.4$ and $J^B/J = 0$. The magnetization-temperature curves are depicted in figure (4).

By comparison with the experimentally measured magnetization temperature curves of $La_{1-x}Ca_xMnO_3$ [12] depicted in Fig.4, we find that our calculations for system M_1 reproduce to grate extend the experimental magnetization-temperature curve for $x = 0.50$, those for M_2 are in good agreement when $x = 0.52$ and system M_3 qualitatively match the experimental curve at $x = 0.55$. The differences are in the tails when the temperature reaches the critical value. They are consequence of the weak magnetic field $H = 4T$ applied during the measurement which makes the slope of the curve $M(T)$ flater. It is not accounted for in the calculations.

The M_1 curve coincides with the experimental one of $Pr_{1-x}Sr_xMnO_3$ [11] for $x = 0.5$. Finally, all three curves reproduce the results for $Pr_{1-x}Gd_xB_4$ [8] when $x = 0.2$, $x = 0.22$ and $x = 0.25$. This suggests that applying magnetic field during preparation of $La_{1-x}Ca_xMnO_3$ one can destroy the AFM-FM transition.

3. Conclusion

In conclusion, we have studied the antiferromagnetic to ferromagnetic phase transition as a transition to partial ordering of spins triggered by charge ordering. As example we have considered multivalent manganites $La_{1-x}Ca_xMnO_3$. When $x < 0.5$ the system undergoes paramagnetic to ferromagnetic phase transition [12]. The phase diagram of $La_{1-x}Ca_xMnO_3$ in the doping range $x < 0.50$ is theoretically studied in [13]. Charge ordered state emerges in the doping range $x \geq 0.50$. It introduces two sublattices A and B and all sites of A are occupied by manganese ions in Mn^{3+} state, so that manganese e_g mobile electrons occupy sublattice A. At $x = 0.5$ the system undergoes transition to charge ordered state accompanied with FM-AFM transition. Experiments [12] show that decreasing the temperature the system undergoes paramagnetic to ferromagnetic phase transition. Our calculations have supplemented this result with the conclusion that only sublattice A spins contribute the magnetisation thereby the ferromagnetic phase is partial ordered state. The magnetization increases with decreasing temperature, reaching its maximum value at T_N . Below Néel temperature it abruptly falls to zero. Our result have added that in this phase the system has two magnons with antiferromagnetic linear dispersion and all spins of the system contribute magnetization. Hence, the ferromagnetism to antiferromagnetism phase transition is partial ordered transition.

When the doping x is increased, the experiment shows that the shape of magnetisation temperature curve changes. Upon cooling the magnetisation increases reaching the maximum at T_N . Below this temperature the magnetisation decreases slowly approaching zero at low temperature. This means that the total magnetization is not zero. Our results have demonstrated that the system has two antiferromagnetic magnons, hence the system is in noncompensated antiferromagnetic phase.

The theoretical studies have reproduced very well the nontrivial fact that the transition from ferromagnetism to antiferromagnetism changes into a

transition from ferromagnetism to uncompensated antiferromagnetism when x increases.

The experimental magnetization-temperature curves for $Pr_{1-x}Gd_xB_4$ [8] and $Pr_{1-x}Sr_xMnO_3$ [11] match very well the theoretical reported in the present paper.

The partial order transition has been observed in Ca_3CoRhO_6 [25, 26] compound which contains one-dimensional chains with ferromagnetic exchange in the chain and antiferromagnetic between chains. The temperature dependence of the magnetization shows a sharp drop at $35K$ in the case of ZFC compounds. For FC materials, the magnetization does not show any such sharp drops, approaching the constant value. Therefore, applying a magnetic field during preparation of the material destroys the partial order transition. This suggests that applying magnetic field during preparation of $La_{1-x}Ca_xMnO_3$ one can destroy the AFM-FM transition.

References

- [1] Cheng Tan, Ji-Hai Liao, Guolin Zheng, Meri Algarni, Jia-Yi Lin, Xiang Ma, Edwin L. H. Mayes, Matthew R. Field, Sultan Albarakati, Majid Panahandeh-Fard, Saleh Alzahrani, Guopeng Wang, Yuanjun Yang, Dimitrie Culcer, James Partridge, Mingliang Tian, Bin Xiang, Yu-Jun Zhao² and Lan Wang, Phys. Rev. Lett. **131**, 166703 (2023).
- [2] Minoru Kinoshita, Mol. Cryst. Liq. Cryst **334**, 229 (1999).
- [3] Valentin Taufour, Udhara S. Kaluarachchi, Rustem Khasanov, Manh Cuong Nguyen, Zurab Guguchia, Pabitra Kumar Biswas, Pietro Bonfà, Roberto De Renzi, Xiao Lin, Stella K. Kim, Eun Deok Mun, Hyunsoo Kim, Yuji Furukawa, Cai-Zhuang Wang, Kai-Ming Ho,^{1,2} Sergey L. Bud'ko, and Paul C. Canfield, Phys. Rev. Lett. **117**, 037207 (2023).
- [4] Udhara S. Kaluarachchi, Sergey L. Bud'ko¹, Paul C. Canfield, and Valentin Taufour, Nature Communications, **8**, 546 (2017).
- [5] Hong-Shuo Li, J.M. Cadogan, X.L. Zhao and S.J. Campbell, Hyperfine Interactions **94**, 1943 (1994).

- [6] S. Hameed, S. El-Khatib, K. P. Olson, B. Yu, T. J. Williams, T. Hong, Q. Sheng, K. Yamakawa, J. Zang, Y. J. Uemura, G. Q. Zhao, C. Q. Jin, L. Fu, Y. Gu, F. Ning, Y. Cai, K. M. Kojima, J. W. Freeland, M. Matsuda, C. Leighton, and M. Greven, *Phys. Rev.* **B 104**, 024410 (2021).
- [7] Shinya Tajiri and Jun-ichiro Inoue, *Phys. Rev.***B 73**, 092411 (2006).
- [8] Toshihiko Kobayashi, Tetsuro Ikemoto, Ryuta Watanuki and Kazuya Suzuki, *Journal of Physics: Conference Series* **176**, 012040 (2009).
- [9] Le Dang Khoi, P Veilleux, J Schaf and I A Campbell, *J. Phys. F: Met. Phys.* **12**, 2055 (1982).
- [10] Jiri Pospisil, Yoshinori Haga, Shinsaku Kambe, Yo Tokunaga, Naoyuki Tateiwa, Dai Aoki, Fuminori Honda, Ai Nakamura, Yoshiya Homma, Etsuji Yamamoto, and Tomoo Yamamura, *Phys. Rev.* **B 95**, 155138 (2017).
- [11] Y. Tomioka, A. Asamitsu, Y. Moritomo, H. Kuwahara, and Y. Tokura, *Phys. Rev. Lett.* **74**, 5108 (1995).
- [12] P. Schiffer, A. P. Ramirez, W. Bao, and S.-W. Cheong, *Phys. Rev. Lett.* **75**, 3336 (1995).
- [13] V. Michev and N. Karchev *Eur. Phys. J.* **B 85**, 177 (2012).
- [14] D. Belitz and T. R. Kirkpatrick, *Phys. Rev. Lett.* **119**, 267202 (1995).
- [15] Marcin M. Wysokiński , *Phys. Rev.* **B 97** ,041107(R) (2018).
- [16] Marcin M. Wysokiński, *Scientific Reports* **9**,19461 (2019).
- [17] V. G. Vaks, A. I. Larkin, and Y. N. Ovchinnikov, *JETP Lett.***22**, 820 1966.
- [18] P. Azaria, H. T. Diep, and H. Giacomini, *Phys. Rev. Lett.* **59**, 1629 1987.
- [19] H. T. Diep (ed.) *Frustrated Spin Systems* World Scientific, Singapore (2004).

- [20] R. Quartu, H. T. Diep, Phys. Rev., **B 55**, 2975 (1997).
- [21] Naoum. Karchev, Phys. Rev. **B 77**, 012405 (2008).
- [22] N. Karchev, JMMM **396**, 77 (2015).
- [23] Supplementary material.
- [24] M. Takahashi, Phys. Rev. Lett. **58**, 168 (1987).
- [25] H. Kageyama, K. Yoshimura, and K. Kosuge, J. Solid State Chem. **140**, 14 (1998).
- [26] Seiji Niitaka, Hiroshi Kageyama, Masaki Kato, Kazuyoshi Yoshimura, and Koji Kosuge, J. Solid State Chem. **146**, 137 (1999).

Antiferromagnetic to ferromagnetic phase transition as a transition to partial ordered spins. Application to $La_{1-x}Ca_xMnO_3$ in the doping range $x \geq 0.50$. Supplementary material to the manuscript

Antiferromagnetism to ferromagnetism transition as a transition to partial ordered spins. Application to $La_{1-x}Ca_xMnO_3$ in the doping range $x \geq 0.50$.

N. Karchev

Department of Physics, Sofia University, James Bourchier 5 blvd., 1164 Sofia, Bulgaria

Abstract

The calculations leading to the results in the main paper are presented.

We consider Heisenberg model of two sublattice spin system with antiferromagnetic nearest neighbors exchange (J) of sublattice A and B spins and two different ferromagnetic exchange constants for sublattice A (J^A) and B (J^B) spins. The Hamiltonian of the system is

$$H = J \sum_{\langle ij \rangle} \mathbf{S}_i^A \cdot \mathbf{S}_j^B \quad (26)$$
$$- J^A \sum_{\langle\langle ij \rangle\rangle_A} \mathbf{S}_i^A \cdot \mathbf{S}_j^A - J^B \sum_{\langle\langle ij \rangle\rangle_B} \mathbf{S}_i^B \cdot \mathbf{S}_j^B$$

where ($\mathbf{S}^A, \mathbf{S}^B$) are spin $s = 3/2$ operators, the sums are over all sites of a body-centered cubic (bcc) lattice. To be specific we choose ($J^A > J^B$). We

Email address: naoum@phys.uni-sofia.bg ()

introduce Holstein-Primakoff representation for the spin operators $\mathbf{S}_j^A(a^+, a)$,

$$\begin{aligned} S_j^{A+} &= S_j^{A1} + iS_j^{A2} = \sqrt{2s - a_j^+ a_j} \ a_j \\ S_j^{A-} &= S_j^{A1} - iS_j^{A2} = a_j^+ \sqrt{2s - a_j^+ a_j} \\ S_j^{A3} &= s - a_j^+ a_j \end{aligned} \quad (27)$$

and $\mathbf{S}_j^B(b^+, b)$,

$$\begin{aligned} S_j^{B+} &= S_j^{B1} + iS_j^{B2} = -b_j^+ \sqrt{2s - b_j^+ b_j} \\ S_j^{B-} &= S_j^{B1} - iS_j^{B2} = -\sqrt{2s - b_j^+ b_j} \ b_j \\ S_j^{B3} &= -s + b_j^+ b_j. \end{aligned} \quad (28)$$

The operators a_j^+ , a_j and b_j^+ , b_j satisfy the Bose commutation relations. In terms of the Bose operators and keeping only the quadratic and quartic terms, the effective Hamiltonian Eq.(26) adopts the form

$$H = H_2 + H_4 \quad (29)$$

where

$$\begin{aligned} H_2 &= sJ^A \sum_{\langle\langle ij \rangle\rangle_A} (a_i^+ a_i + a_j^+ a_j - a_j^+ a_i - a_i^+ a_j) \\ &+ sJ^B \sum_{\langle\langle ij \rangle\rangle_B} (b_i^+ b_i + b_j^+ b_j - b_j^+ b_i - b_i^+ b_j) \\ &+ sJ \sum_{\langle ij \rangle} [b_j^+ b_j + a_i^+ a_i - (a_i^+ b_j^+ + a_i b_j)] \end{aligned} \quad (30)$$

and

$$\begin{aligned} H_4 &= \frac{1}{4} J^A \sum_{\langle\langle ij \rangle\rangle_A} [a_i^+ a_j^+ (a_i - a_j)^2 + (a_i^+ - a_j^+)^2 a_i a_j] \\ &+ \frac{1}{4} J^B \sum_{\langle\langle ij \rangle\rangle_B} [b_i^+ b_j^+ (b_i - b_j)^2 + (b_i^+ - b_j^+)^2 b_i b_j] \\ &+ \frac{1}{4} J \sum_{\langle ij \rangle} [a_i b_j^+ b_j b_j + a_i^+ b_j^+ b_j^+ b_j \\ &+ a_i^+ a_i a_i b_j + a_i^+ a_i^+ a_i b_j^+ - 4a_i^+ a_i b_j^+ b_j]. \end{aligned} \quad (31)$$

The terms without operators are dropped.

The next step is to represent the Hamiltonian in the Hartree-Fock approximation

$$H \approx H_{HF} = H_{cl} + H_q, \quad (32)$$

with

$$\begin{aligned} H_{cl} &= 6NJ^A s^2 (u^A - 1)^2 + 6NJ^B s^2 (u^B - 1)^2 \\ &+ 8NJs^2 (u - 1)^2, \end{aligned} \quad (33)$$

and

$$H_q = \sum_{k \in B_r} \left[\varepsilon_k^a a_k^+ a_k + \varepsilon_k^b b_k^+ b_k - \gamma_k (a_k^+ b_k^+ + b_k a_k) \right], \quad (34)$$

where $N = N^A = N^B$ is the number of sites on a sublattice. The two equivalent sublattices A and B of the bcc lattice are simple cubic lattices. The wave vector k runs over the reduced first Brillouin zone B_r of a bcc lattice which is the first Brillouin zone of a simple cubic lattice.

The dispersions are given by equalities

$$\begin{aligned} \varepsilon_k^a &= 4sJ^A u^A (3 - \cos k_x - \cos k_y - \cos k_z) + 8sJu \\ \varepsilon_k^b &= 4sJ^B u^B (3 - \cos k_x - \cos k_y - \cos k_z) + 8sJu \\ \gamma_k &= 8Jus \cos \frac{k_x}{2} \cos \frac{k_y}{2} \cos \frac{k_z}{2} \end{aligned} \quad (35)$$

The equations (35) show that Hartree-Fock parameters (u^A, u^B, u) renormalize the intra and inter-sublattice exchange constants (J^A, J^B, J) respectively.

To diagonalize the Hamiltonian one introduces new Bose fields $\alpha_k, \alpha_k^+, \beta_k, \beta_k^+$ by means of the transformation

$$\begin{aligned} a_k &= u_k \alpha_k + v_k \beta_k^+ & a_k^+ &= u_k \alpha_k^+ + v_k \beta_k \\ b_k &= u_k \beta_k + v_k \alpha_k^+ & b_k^+ &= u_k \beta_k^+ + v_k \alpha_k, \end{aligned} \quad (36)$$

where the coefficients of the transformation u_k and v_k are real functions of the wave vector k :

$$u_k = \sqrt{\frac{1}{2} \left(\frac{\varepsilon_k^a + \varepsilon_k^b}{\sqrt{(\varepsilon_k^a + \varepsilon_k^b)^2 - 4\gamma_k^2}} + 1 \right)}$$

(37)

$$v_k = \text{sign}(\gamma_k) \sqrt{\frac{1}{2} \left(\frac{\varepsilon_k^a + \varepsilon_k^b}{\sqrt{(\varepsilon_k^a + \varepsilon_k^b)^2 - 4\gamma_k^2}} - 1 \right)}.$$

The transformed Hamiltonian adopts the form

$$H_q = \sum_{k \in B_r} \left(E_k^\alpha \alpha_k^+ \alpha_k + E_k^\beta \beta_k^+ \beta_k + E_k^0 \right), \quad (38)$$

with new dispersions

$$E_k^\alpha = \frac{1}{2} \sum_{k \in B_r} \left[\sqrt{(\varepsilon_k^a + \varepsilon_k^b)^2 - 4\gamma_k^2} - \varepsilon_k^b + \varepsilon_k^a \right]$$

$$E_k^\beta = \frac{1}{2} \sum_{k \in B_r} \left[\sqrt{(\varepsilon_k^a + \varepsilon_k^b)^2 - 4\gamma_k^2} + \varepsilon_k^b - \varepsilon_k^a \right]$$

and vacuum energy

$$E_k^0 = \frac{1}{2} \left[\sqrt{(\varepsilon_k^a + \varepsilon_k^b)^2 - 4\gamma_k^2} - \varepsilon_k^b - \varepsilon_k^a \right] \quad (39)$$

For positive values of the Hartree-Fock parameters and all values of $k \in B_r$, the dispersions are nonnegative $E_k^\alpha \geq 0$, $E_k^\beta \geq 0$. The α_k and β_k bosons are the long-range (**magnon**) excitations with linear dispersion $E_k^\alpha \propto c^\alpha |k|$ and $E_k^\beta \propto c^\beta |k|$, near the zero wave vector. For spin velocity constants we obtained

$$c^\alpha = c^\beta = 4s \sqrt{Ju (J^A u^A + J^B u^B + Ju)}. \quad (40)$$

The free energy of a system with Hamiltonian H_{HF} equations (32), (33) and (34) is

$$\begin{aligned} \mathcal{F} &= 6N J^A s^2 (u^A - 1)^2 + 6N J^B s^2 (u^B - 1)^2 \\ &+ 8N J s^2 (u - 1)^2 + \frac{1}{N} \sum_{k \in B_r} E_k^0 \\ &+ \frac{1}{\beta N} \sum_{k \in B_r} \left[\ln(1 - e^{-\beta E_k^\alpha}) + \ln(1 - e^{-\beta E_k^\beta}) \right], \end{aligned} \quad (41)$$

where $\beta = 1/T$ is the inverse temperature. Then, the system of equations for the Hartree-Fock parameters is

$$\partial\mathcal{F}/\partial u^A = 0, \quad \partial\mathcal{F}/\partial u^B = 0, \quad \partial\mathcal{F}/\partial u = 0. \quad (42)$$

One can write them by means of the Bose functions n_k^α and n_k^β of α and β excitations.

$$\begin{aligned} u^A &= 1 - \frac{1}{3s} \frac{1}{N} \sum_{k \in B_r} \varepsilon_k \left[u_k^2 n_k^\alpha + v_k^2 n_k^\beta + v_k^2 \right] \\ u^B &= 1 - \frac{1}{3s} \frac{1}{N} \sum_{k \in B_r} \varepsilon_k \left[v_k^2 n_k^\alpha + u_k^2 n_k^\beta + v_k^2 \right] \\ u &= 1 - \frac{1}{N} \sum_{k \in B_r} \left[\frac{1}{2s} \left(u_k^2 n_k^\alpha + v_k^2 n_k^\beta + v_k^2 \right) \right. \\ &\quad \left. + \frac{1}{2s} \left(v_k^2 n_k^\alpha + u_k^2 n_k^\beta + v_k^2 \right) \right. \\ &\quad \left. - 8Ju \left(1 + n_k^\alpha + n_k^\beta \right) \frac{\left(\cos \frac{k_x}{2} \cos \frac{k_y}{2} \cos \frac{k_z}{2} \right)^2}{\sqrt{(\varepsilon_k^a + \varepsilon_k^b)^2 - 4\gamma_k^2}} \right] \end{aligned} \quad (43)$$

The Hartree-Fock parameters are positive functions of T/J , solution of the system of equations (42) (see Eqs.(43)). Utilizing these functions, one can calculate the spontaneous magnetization on the two sublattices

$$M^A = \langle S_j^{A3} \rangle \quad j \text{ is from sublattice } A \quad (44)$$

$$M^B = \langle S_j^{B3} \rangle \quad j \text{ is from sublattice } B$$

and $M = M^A + M^B$, the spontaneous magnetization of the system. In terms of the Bose functions

$$\begin{aligned} M^A &= s - \frac{1}{N} \sum_{k \in B_r} \left[u_k^2 n_k^\alpha + v_k^2 n_k^\beta + v_k^2 \right] \\ M^B &= -s + \frac{1}{N} \sum_{k \in B_r} \left[v_k^2 n_k^\alpha + u_k^2 n_k^\beta + v_k^2 \right], \end{aligned} \quad (45)$$

where u_k and v_k are functions of the wavevector k , coefficients in the transformation (36).

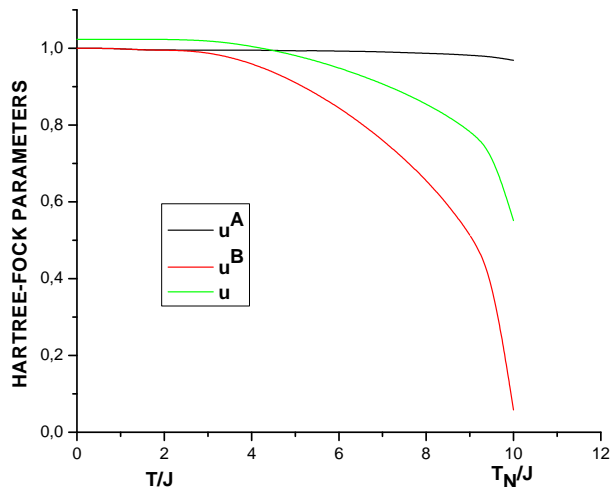


Figure 5: The Hartree-Fock parameters are depicted, as a function of dimensionless temperature T/J within the interval $(0, T_N/J)$, for a system with parameters $J^A/J = 0.8$ and $J^B/J = 0.006$.

The Hartree-Fock parameters as functions of T/J within interval $(0, T_N/J)$ are depicted in Fig.(1).

The sublattice A and B magnetization M^A , M^B are depicted in Fig.(2). The magnons' fluctuations suppress in a different way the magnetization on sublattices A and B. Quantitatively this depends on the exchange constants J^A and J^B . At characteristic temperature T_N spontaneous magnetization on sublattice B becomes equal to zero, while spontaneous magnetization on sublattice A is still nonzero Fig.(2). The total magnetization $M^A + M^B$ increases and reaches its maximum value at T_N Fig.(2). The system in the temperature interval $(0, T_N)$ has two antiferromagnetic magnons but sublattice A and B magnetization do not compensate each other. We name this phase noncompensated antiferromagnetic.

Above the Néel temperature the magnetic moments of the sublattice B electrons do not contribute the magnetization of the system. To study this "partial ordered" state we first consider the paramagnetic phase. To this end we make use of the Takahashi modified spin-wave theory [5, 6] and introduce two parameters λ^A and λ^B to enforce the magnetization on the two sublattices to be equal to zero. The new Hamiltonian is obtained from the old one

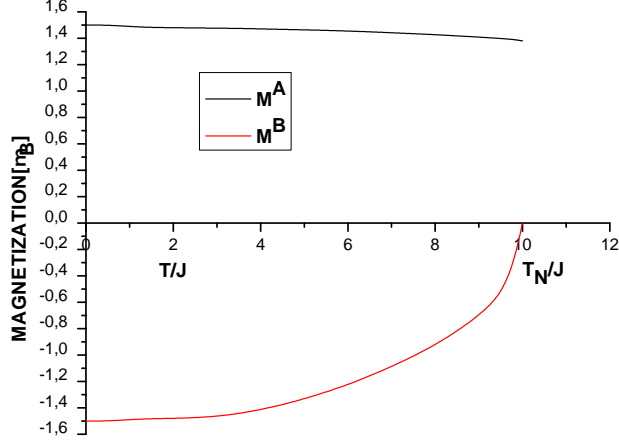


Figure 6: The sublattice A and B magnetization are depicted as a function of dimensionless temperature T/J within the interval $(0, T_N/J)$, for a system with parameters $J^A/J = 0.8$ and $J^B/J = 0.006$.

(26) adding two new terms:

$$\hat{H} = H - \sum_{i \in A} \lambda^A S_i^{A3} + \sum_{i \in B} \lambda^B S_i^{B3}. \quad (46)$$

In momentum space the new Hamiltonian adopts the form

$$\hat{H} = \sum_{k \in B_r} [\hat{\varepsilon}_k^a a_k^+ a_k + \hat{\varepsilon}_k^b b_k^+ b_k - \gamma_k (b_k a_k + b_k^+ a_k^+)] \quad (47)$$

where the new dispersions are

$$\hat{\varepsilon}_k^a = \varepsilon_k^a + \lambda^A, \quad \hat{\varepsilon}_k^b = \varepsilon_k^b + \lambda^B. \quad (48)$$

It is convenient to represent the parameters λ^A and λ^B in the form

$$\lambda^A = 8Jus(\mu^A - 1), \quad \lambda^B = 8Jus(\mu^B - 1). \quad (49)$$

The dispersions $\hat{\varepsilon}_k^a$ and $\hat{\varepsilon}_k^b$ adopt the form

$$\begin{aligned} \hat{\varepsilon}_k^a &= 4sJ^A u^A (3 - \cos k_x - \cos k_y - \cos k_z) + 8sJu\mu^A \\ \hat{\varepsilon}_k^b &= 4sJ^B u^B (3 - \cos k_x - \cos k_y - \cos k_z) + 8sJu\mu^B \end{aligned} \quad (50)$$

They are positive ($\hat{\varepsilon}_k^a > 0$, $\hat{\varepsilon}_k^b > 0$) for all values of the wavevector k , if the parameters μ^A and μ^B are positive ($\mu^A > 0$, $\mu^B > 0$).

To obtain the Hamiltonian (47) in diagonal form, we use a transformation (36,37) replacing ε_k^a and ε_k^b with $\hat{\varepsilon}_k^a$ and $\hat{\varepsilon}_k^b$. The result is

$$\hat{H} = \sum_{k \in B_r} \left(\hat{E}_k^\alpha \alpha_k^\dagger \alpha_k + \hat{E}_k^\beta \beta_k^\dagger \beta_k + \hat{E}_k^0 \right), \quad (51)$$

where

$$\begin{aligned} \hat{E}_k^\alpha &= \frac{1}{2} \left[\sqrt{(\hat{\varepsilon}_k^a + \hat{\varepsilon}_k^b)^2 - 4\gamma_k^2} - \hat{\varepsilon}_k^b + \hat{\varepsilon}_k^a \right] \\ \hat{E}_k^\beta &= \frac{1}{2} \left[\sqrt{(\hat{\varepsilon}_k^a + \hat{\varepsilon}_k^b)^2 - 4\gamma_k^2} + \hat{\varepsilon}_k^b - \hat{\varepsilon}_k^a \right] \\ \hat{E}_k^0 &= \frac{1}{2} \left[\sqrt{(\hat{\varepsilon}_k^a + \hat{\varepsilon}_k^b)^2 - 4\gamma_k^2} - \hat{\varepsilon}_k^b - \hat{\varepsilon}_k^a \right] \end{aligned} \quad (52)$$

The dispersions Eq.(52) are well defined if square-roots in equations (52) are well defined. This is true if

$$\mu^A \mu^B \geq 1. \quad (53)$$

If $\mu^A \mu^B > 1$ the dispersions (52) are positive ($\hat{E}_k^\alpha > 0$, $\hat{E}_k^\beta > 0$). This means that the system is in paramagnetic phase. When $\mu^A \mu^B = 1$ the spectrum of the system posses long-range (magnon) excitation and it is in ordered phase.

In the partial ordered phase above T_N with $M^B = 0$ sublattice A magnetization contributes the total magnetic moment. To study this ordered phase one has to solve a system of four equations, three for Hartree-Fock parameters and one ($M^B = 0$) for $\mu^A = 1/\mu^B$. The solution of the system, the Hartree-Fock parameters and parameters $\mu^A = 1/\mu^B$ as fuctions of T/J within interval $(0, T_C/J)$ are depicted in Fig.(3) and Fig.(4) respectively. Above the T_C , the critical order-disorder transition temperature, one obtains $\mu^A \mu^B > 1$. The sublattice A and B magnetization M^A and M^B are depicted in Fig.(5). The total magnetization $M^A + M^B$ is depicted in Fig.(1) in the main article.

The figure (4) shows that μ^B is larger than μ^A . As a result we obtain that β excitation is gapped ($E_k^\beta > 0$ for all values of the wave vector k), while $E_0^\alpha = 0$ and near the zero wave vector

$$\hat{E}_k^\alpha \approx \hat{\rho} k^2 \quad (54)$$

with spin-stiffness constant

$$\hat{\rho} = s \frac{(\mu^A + \mu^B)(J^A u^A + J^B u^B) + 2JU}{\mu^B - \mu^A} + sJ^A u^A - sJ^B u^B. \quad (55)$$

This means that α_k boson is the long-range excitation (ferromagnetic magnon) in the system.

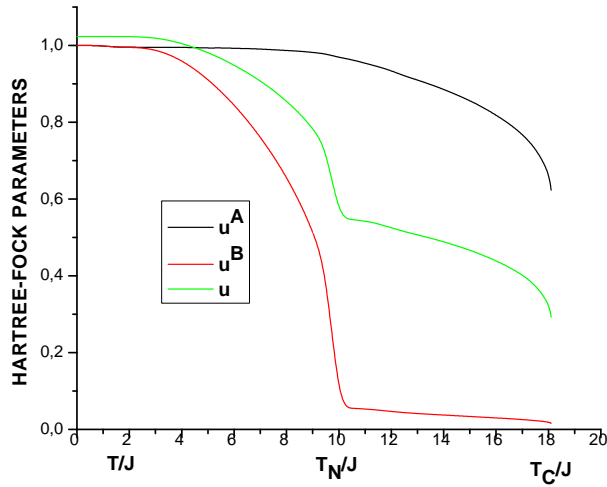


Figure 7: The Hartree-Fock parameters are depicted as a function of dimensionless temperature T/J within the interval $(0, T_C/J)$, for a system with parameters $J^A/J = 0.8$ and $J^B/J = 0.006$.

In conclusion, we will note that in the paramagnetic phase $\mu^A \mu^B > 1$. On decreasing the temperature the product $\mu_1 \mu_2$ decreases, remaining larger than one. At temperature T_C at which the product becomes equal to one ($\mu^A \mu^B = 1$) the system undergoes paramagnetic-ferromagnetic phase transition. Only sublattice A spins contribute the total magnetization, i.e. the ferromagnetic phase is partial ordered phase. Below T_C at T_N , μ^A and μ^B become equal to one ($\mu^A = \mu^B = 1$) and the system undergoes ferromagnetic to noncompensated antiferromagnetic phase transition. In the low temperature phase sublattice A and B spins contribute the total magnetization. Hence, ferromagnetic-antiferromagnetic phase transition is a partial ordered transition.

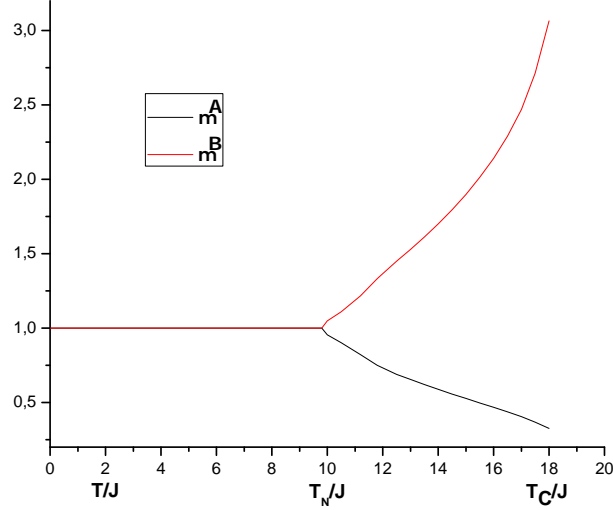


Figure 8: The parameters μ^A and μ^B are depicted as a function of dimensionless temperature T/J within the interval $(0, T_C/J)$, for a system with parameters $J^A/J = 0.8$ and $J^B/J = 0.006$.

It is useful to plot magnon dispersions at different temperatures. The dimensionless dispersions $E^\alpha/2sJ$ and $E^\beta/2sJ$, below T_N are plotted in figure 6 for a system with parameters $J^A/J = 0.8$, $J^B/J = 0.5$ and $T = 0.5T_N$. The dispersions at temperatures above T_N , $T = 1.5T_N$ are plotted in figure 7.

References

- [1] L. P. Gor'kov and G. M. Eliashberg, Soviet Phys. JETP **27**, 328 (1968).
- [2] R. S. Thompson, Phys. Rev. **B 1**, 327 (1970).
- [3] Michael Tinkham, *Introduction to Superconductivity* (McGraw-Hill, Inc, 1975).
- [4] Naoum Karchev, Condens. Matter **2**, 20 (2017)(arXiv:1512.04284).
- [5] M. Takahashi, Phys. Rev. Lett. **58**, 168 (1987).
- [6] Naoum Karchev, Phys. Rev. **B 77**, 012405 (2008).

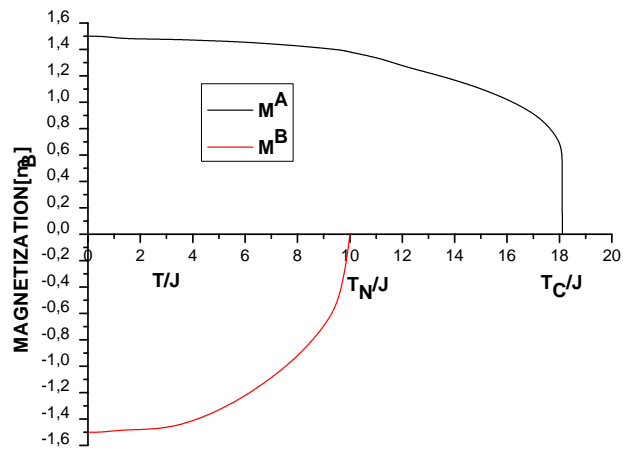


Figure 9: The sublattice A and B magnetization are depicted as a function of dimensionless temperature T/J within the interval $(0, T_C/J)$, for a system with parameters $J^A/J = 0.8$ and $J^B/J = 0.006$.

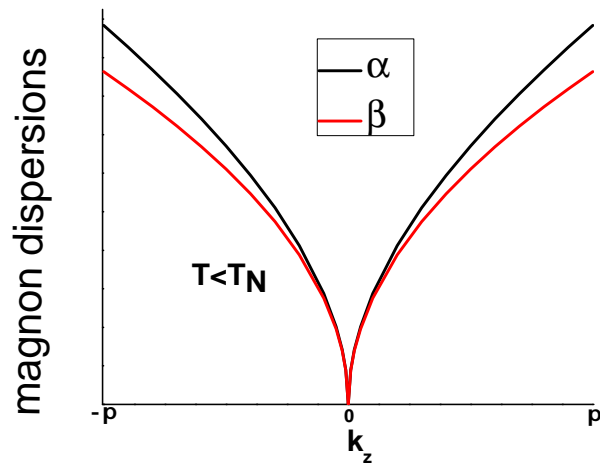


Figure 10: The dimensionless dispersion $E^\alpha/2sJ$ and $E^\beta/2sJ$ are depicted as a function of k_z and $k_x = k_y = 0$, for system with parameters $J^A/J = 0.8$, $J^B/J = 0.5$ and $T = 0.5T_N$

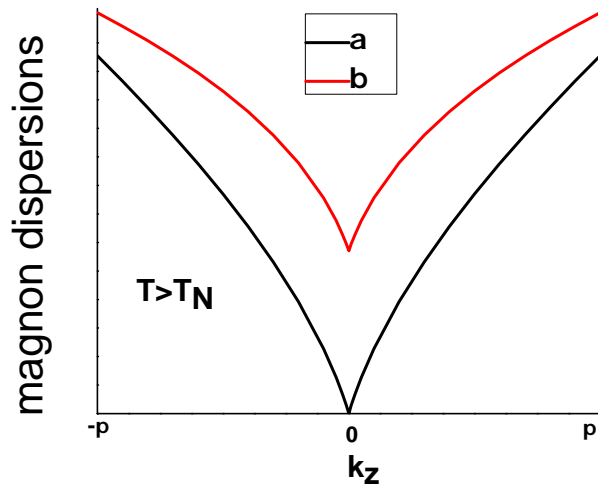


Figure 11: The dimensionless dispersion $E^\alpha/2sJ$ and $E^\beta/2sJ$ are depicted as a function of k_z and $k_x = k_y = 0$, for system with parameters $J^A/J = 0.8$, $J^B/J = 0.5$ and $T = 1.25T_N$